

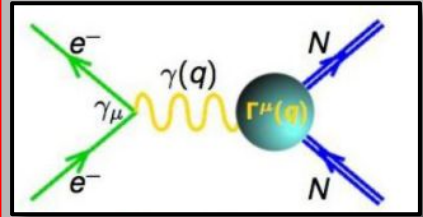
# Measurements of the Neutron Electric Form Factor at High $Q^2$

Gary Penman  
QNP 2024  
11.07.24

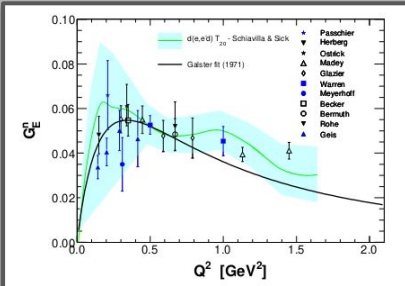
# GEN-II: Neutron Electric Form Factor at High $Q^2$



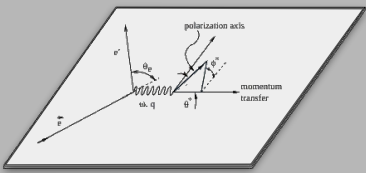
Double polarized semi-exclusive  $^3\text{He}(e, e'n)pp$  quasi-elastic scattering



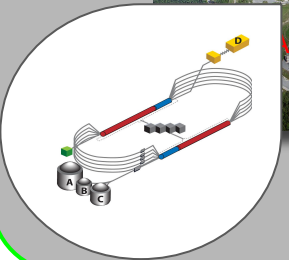
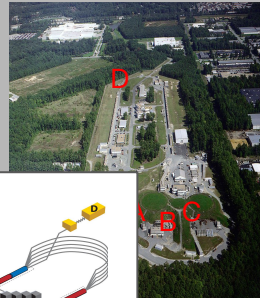
Extract Sachs Form Factor  $G_E^n$  with precise high  $Q^2$  GMn data.



Measure transverse asymmetry  $A_{\perp}$  of cross section



Hall A - Thomas Jefferson National Accelerator Facility



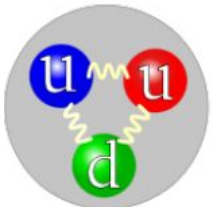
# Elastic eN Scattering and Form Factors

R. Hofstadter et al. (1950s)

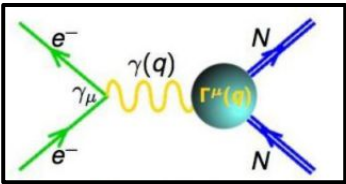
$$\sigma(\theta_e) = \sigma_M \left| \int \rho(r) e^{iq \cdot r} d^3r \right|^2 = \sigma_M |F(q)|^2$$

$$\begin{aligned} F_{1p}(0) &= 1 & \kappa_p &= \mu_p - 1 \\ F_{2p}(0) &= \kappa_p \\ F_{1n}(0) &= 0 & \kappa_n &= \mu_n \\ F_{2n}(0) &= \kappa_n \end{aligned}$$

$Q^2 = 0$

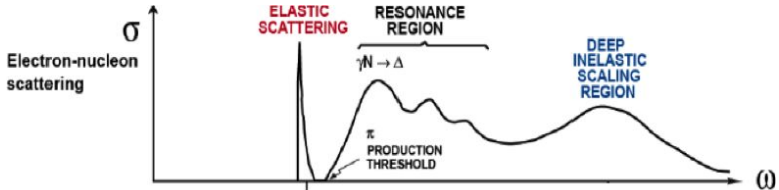
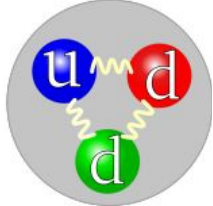


$Q^2 = (\bar{q} - q)^2$

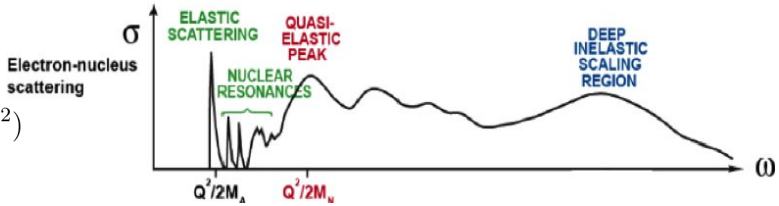


Born Term:

$$\Gamma_\mu(p, p') = \gamma_\mu F_1(Q^2) + \frac{i\sigma_{\nu\mu}}{2M} F_2(Q^2)$$



$F_1$ : helicity non-conserving, Pauli FF  
 $F_2$ : helicity conserving, Dirac FF



F.J. Ernst et al (1960s)

$$\begin{aligned} G_E &= F_1 - \frac{Q^2}{M^2} F_2 \\ G_M &= F_1 + F_2 \end{aligned}$$

$$\frac{d\sigma}{d\Omega} = \frac{\alpha^2}{4E^2 \sin^4 \theta/2} \frac{E}{E'} \left[ \frac{G_E^2 + \tau G_M^2 \cos^2 \theta/2 + 2\tau G_M^2 \sin^2 \theta/2}{1 + \tau} \right]$$

point-like target      Electric form-factor      Magnetic form-factor

$$\tau \equiv \frac{Q^2}{4M^2}$$

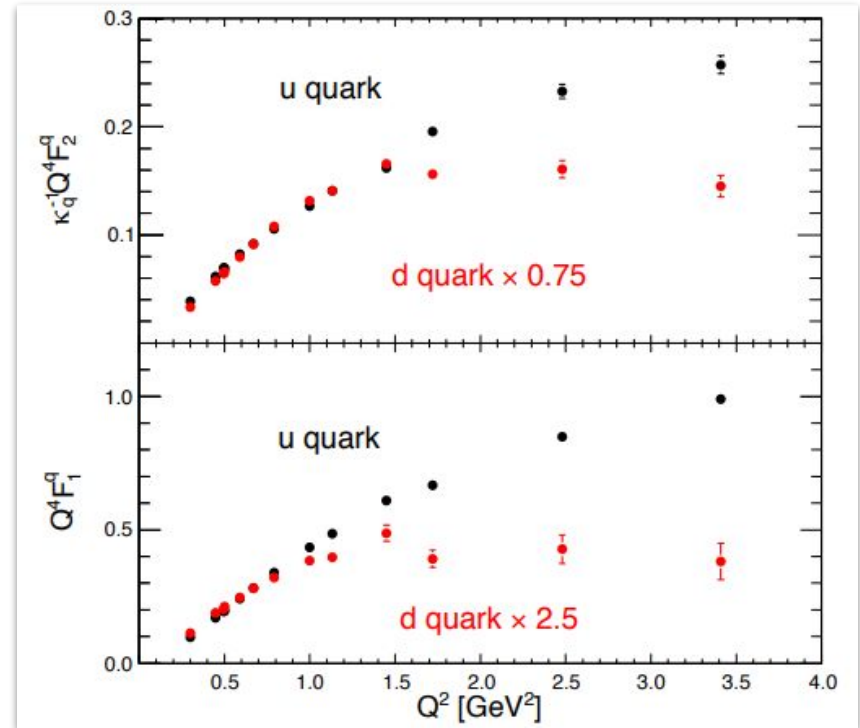
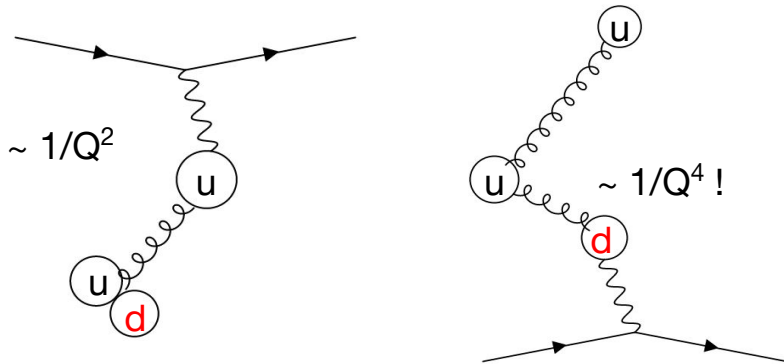
Nucleon structure is revealed in the  $Q^2$  evolution of the form factors

# Flavour Separation

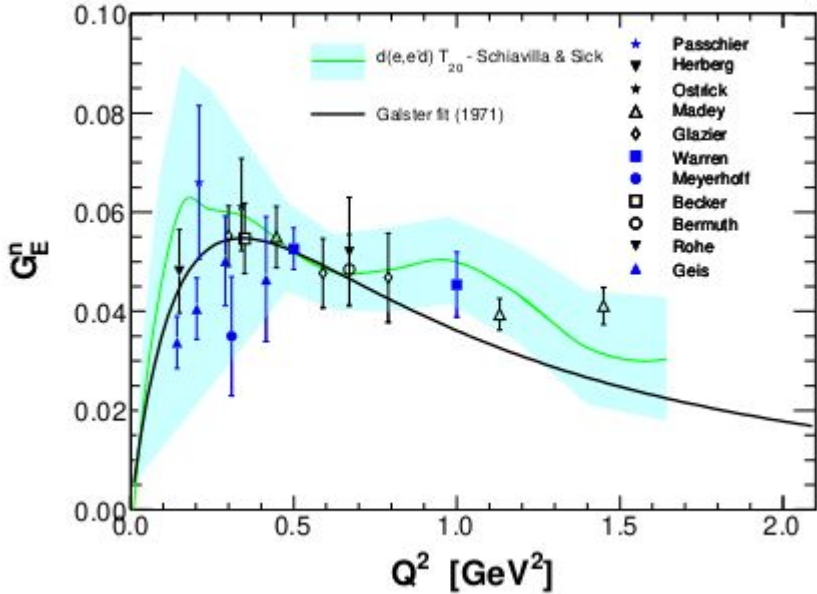
Extracted  $G_E$  and  $G_M$  can be decomposed

$$F_1 = \frac{G_E + \tau G_M}{1 + \tau} \quad F_2 = -\frac{G_E - G_M}{1 + \tau}$$

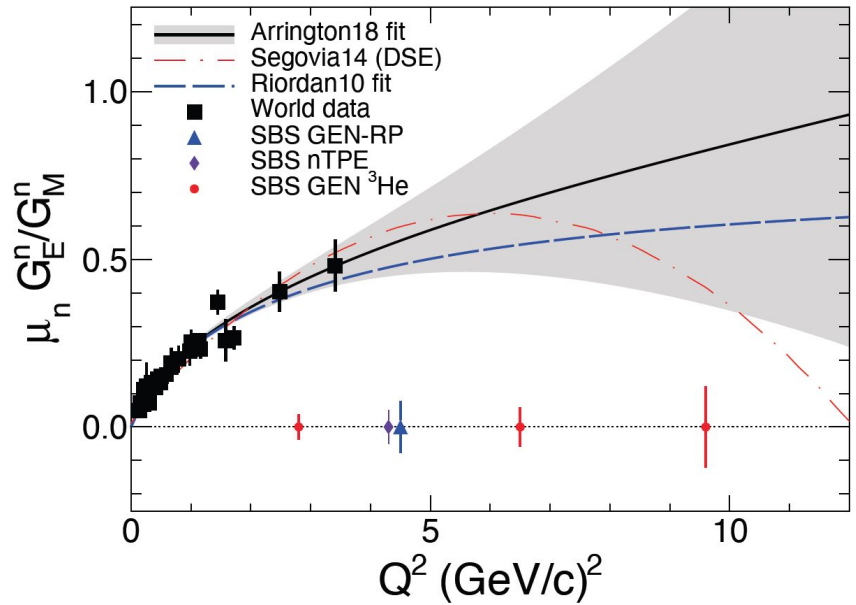
Different behaviour of u and d quarks may indicate diquark correlations



# Electric Form Factor of the Neutron ( $G_E^n$ )



World data for  $G_E^n$  from polarized measurements

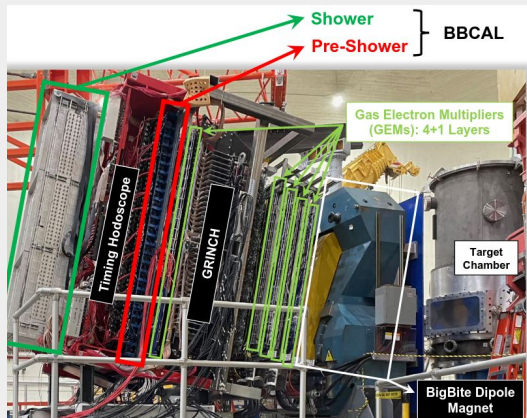


Projected points for GEN-II experiment (red), credit A. J. R. Puckett (2023)

# Hall A Experimental Setup: Super Bigbite Spectrometer

## Electron Arm: Bigbite

- 750A Dipole Magnet
- Full Detector Stack
  - Calo Trigger
  - GEM Tracking
  - Cherenkov
  - Timing
  - Hodoscope



## Nucleon Arm: SBS

- 2100A Dipole Magnet
- Hadron Calorimeter



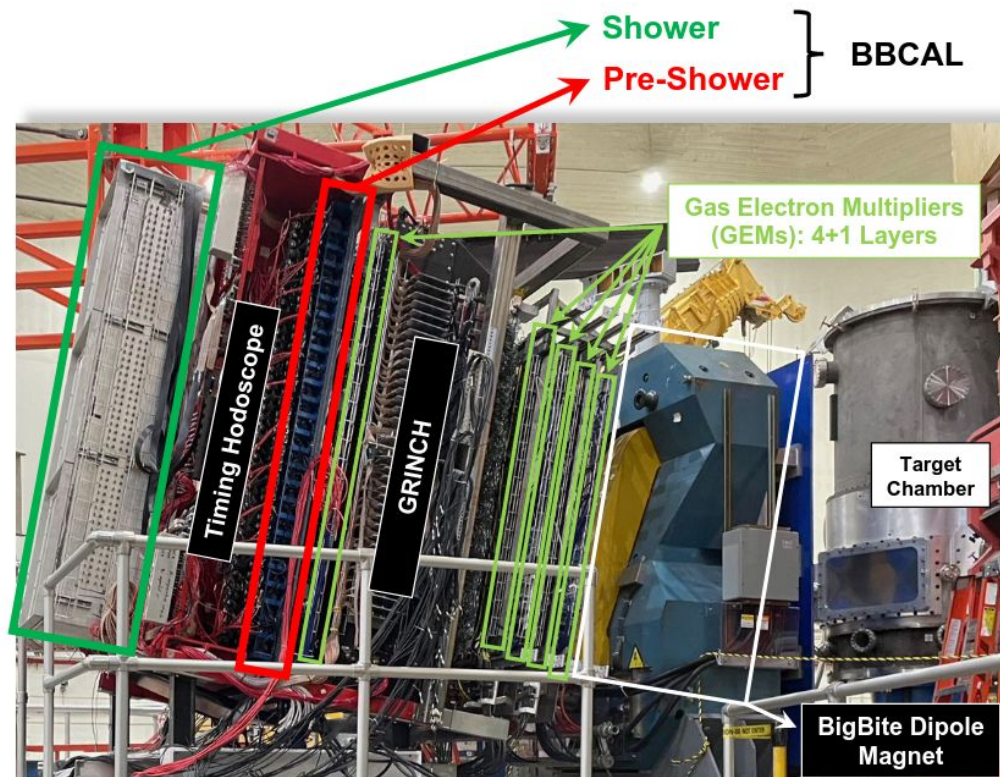
## Polarised $^3\text{He}$ Target



# Electron Arm: Bigbite

- Bigbite magnet
- (4 Front UV + 1 Rear XY) gas electron multiplier (GEM) tracking layers.
- Gas Cherenkov (GRINCH) detector
- Preshower Calorimeter (2x26 lead-glass blocks)
- Timing Hodoscope (89bars + 178pmts)
- Shower Calorimeter (7x27 lead-glass blocks)

BBCAL forms single arm trigger. Analogue “OR” sum of energy deposited in 26 trigger modules.



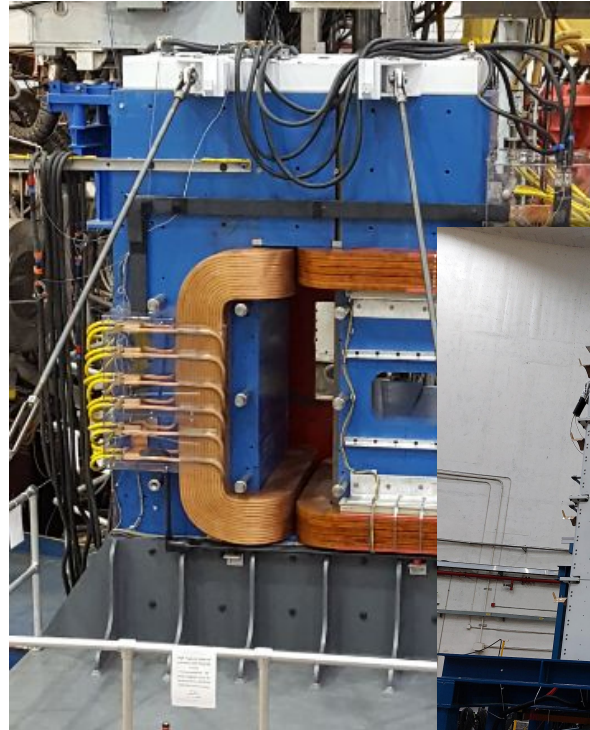
P. Datta (FC NHP 2022)

[https://indico.ilab.org/event/529/contributions/10270/attachments/8180/11693/F%26C\\_MIT\\_gmn%26bbcal\\_2022.pdf](https://indico.ilab.org/event/529/contributions/10270/attachments/8180/11693/F%26C_MIT_gmn%26bbcal_2022.pdf)

# Nucleon Arm: Super Bigbite

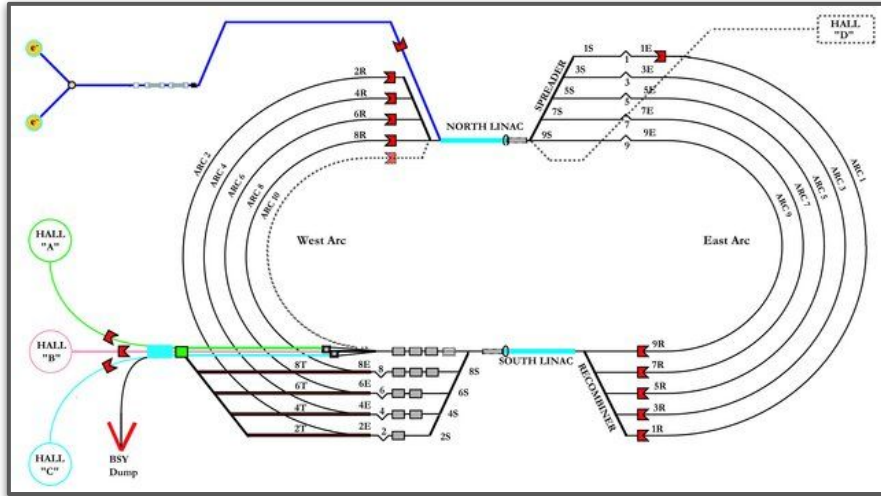
- **SBS Magnet**
  - 2100A at 100% - p,n separation!
- (2INFN + 6UVa) GEM layers
  - Fully utilised in GEP Experiment
- **Hadron Calorimeter [HCAL] (242 Fe/Scintillator plate blocks)**
  - ~700ps TOF and ~30% energy resolution

HCAL + BBCAL function as coincidence trigger

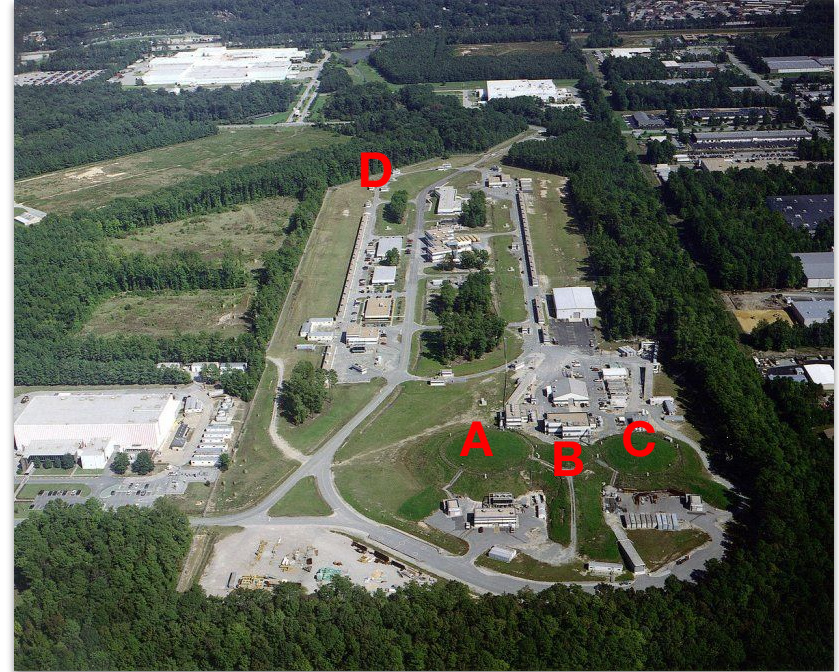




# CEBAF: Continuous Electron Beam Accelerator Facility



Linearly polarised electron beams up to 12 GeV and around 85% polarisation to four experimental halls simultaneously



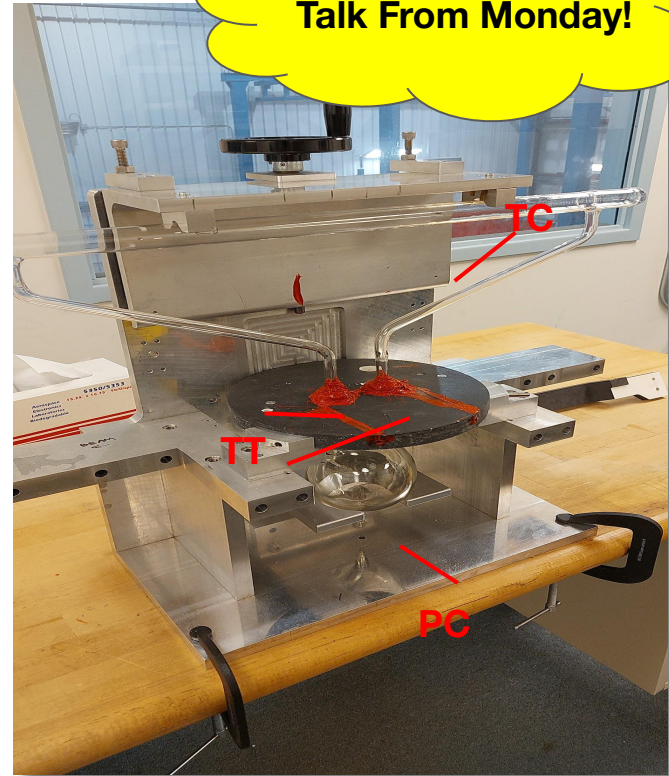
# Polarised $^3\text{He}$ Target

10 atm glass 'cell' comprised of pumping chamber (PC), transfer tubes (TT) and target chamber (TC).

PC Filled with  $^3\text{He}$ ,  $\text{N}_2$ , and 2 alkali metals (K-19 and Rb-85)

PC resides inside ceramic 'oven' at around 260 degrees C.

High power narrowband lasers directed onto TC via mirror system

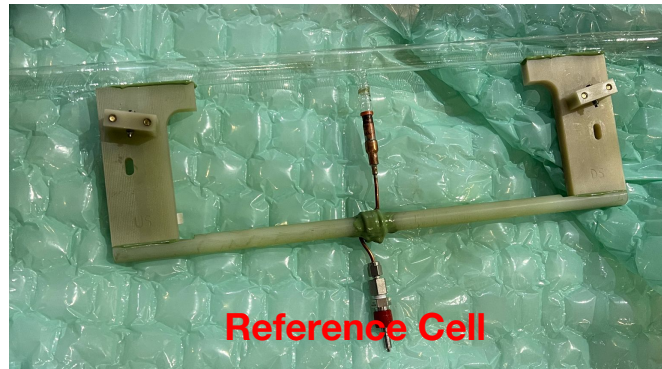


# Polarised $^3\text{He}$ Target

Entire system located within set of Helmholtz (HH) coils.

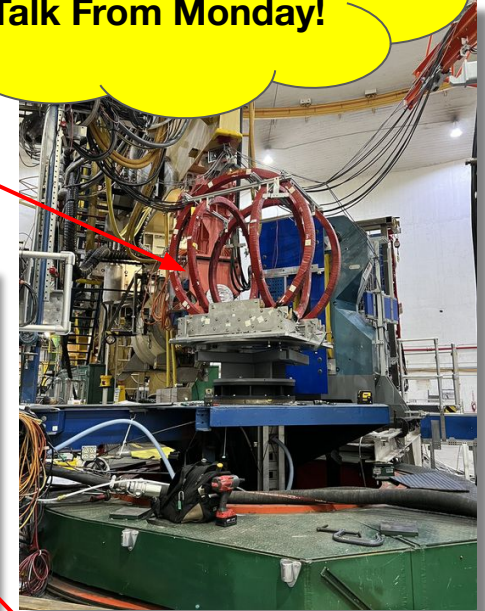
Downstream transfer tube has heater strip to induce convection around cell.

$^3\text{He}$  gas polarised via spin exchange optical pumping (SEOP).



Rotate to match magnets

See A. Tadepalli  
Talk From Monday!



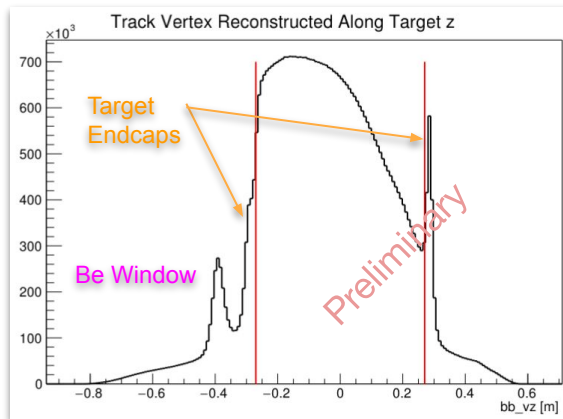
RTDs for Temp monitoring

# Analysis: $e^-$ Track Selection

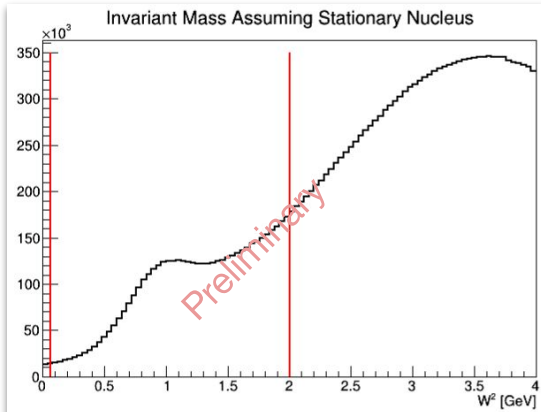
Tracking Performed by Gas Electron Multipliers (GEMs)

Calorimeter trigger provides a track search region.  
Track algorithm finds all possible tracks with at least 3 hits within the 5 GEM layers

Track Algorithm produces a “best track” per event with 99%+ efficiency



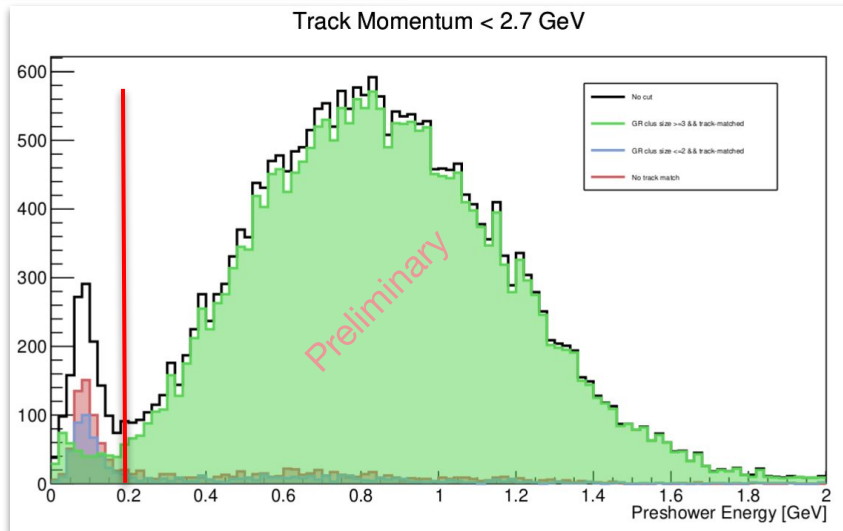
Remove scattering associated with target and beryllium beam-pipe window.



A wide starting cut around the nucleon mass squared, 0.88 GeV<sup>2</sup> removes superelastic & most inelastic events

## $\pi^-$ rejection

$\pi^-$  and  $e^-$  exhibit clear and different behaviors in the preshower calorimeter and GRINCH cherenkov detector in energy deposition and cluster size respectively



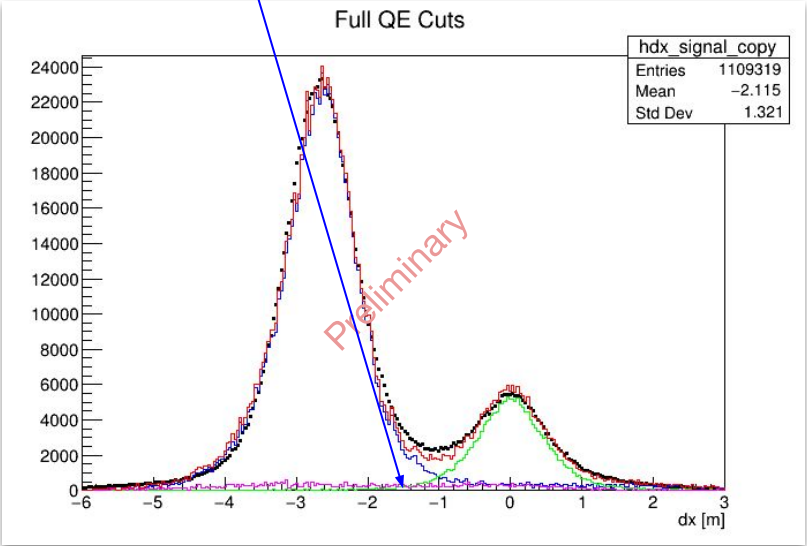
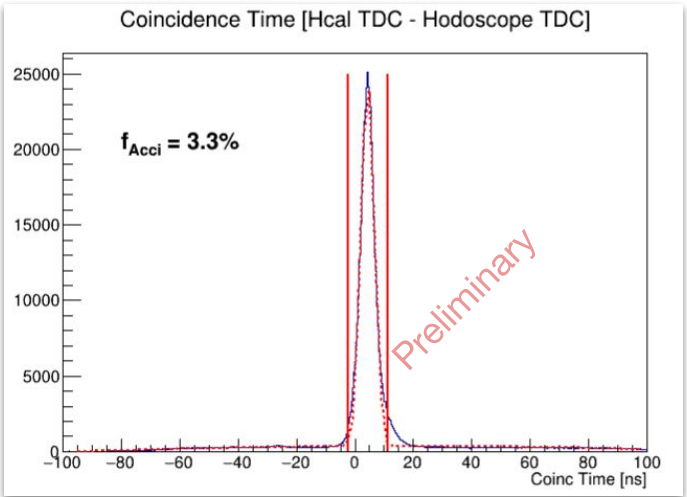
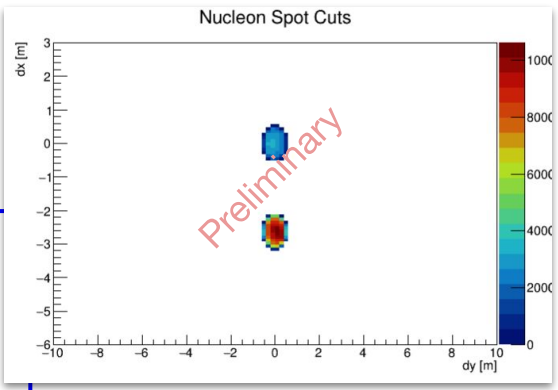
# Exclusive Nucleon Selection

Demand coincidence trigger between Bigbite and SBS.

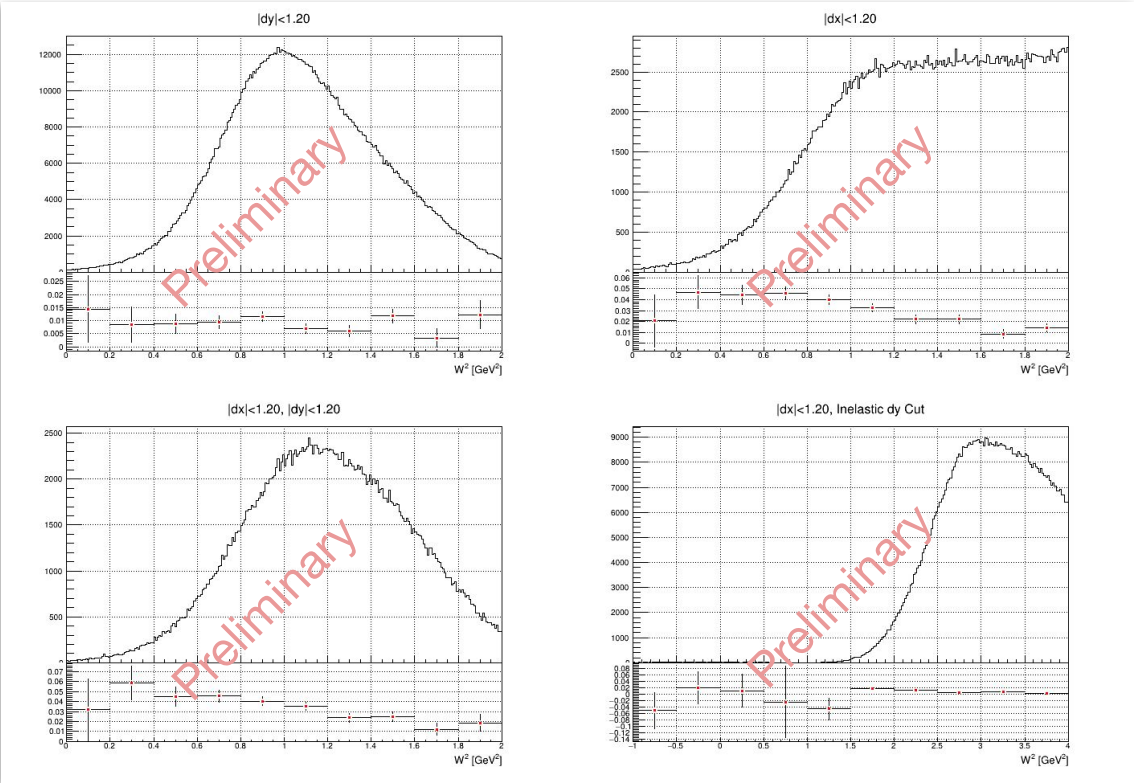
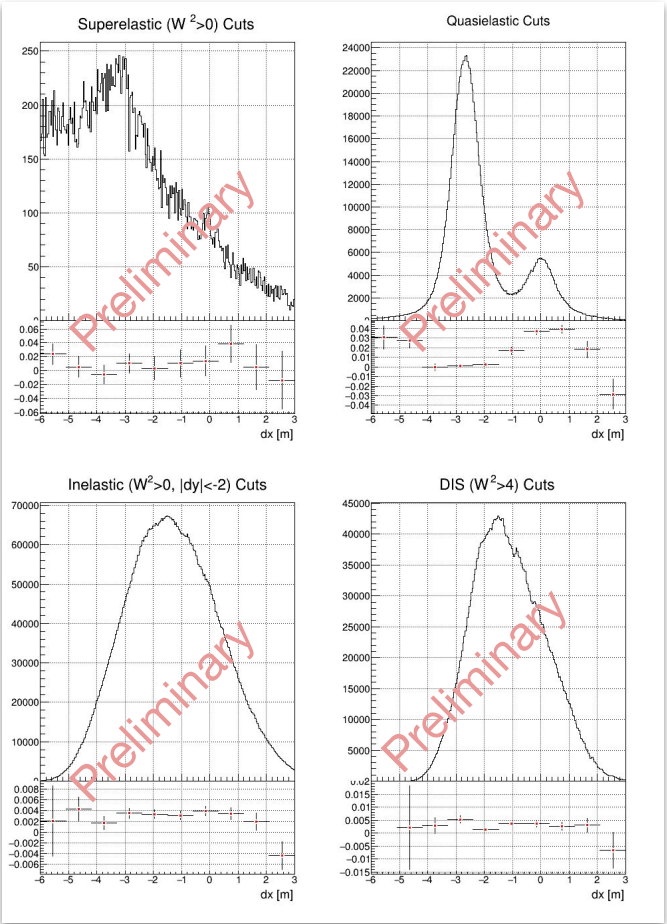
Project q-vector towards HCal.

Quasi-elastic position projected-detected cuts (dx, dy) select on QE spots

Fit dx shape with Signal and Background MC Sims -> Good Estimation of background shape and fraction



# Preliminary Asymmetries and Backgrounds

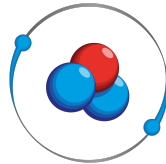


In Progress analysis of background fractions and associated dilution asymmetries

# Conclusion & Next Steps

- ❖ Pass 2 data requirements (among other things)
  - Calorimeter re-calibration on neutron data
  - Inclusion of Cherenkov calibrated database
  - Recalibration of timing
- ❖ Finalise Thesis Analysis
  - In the process of writing up *internal results* into thesis. Stay tuned!
- ❖ Publication
  - Full analysis likely a few years more progress. Pass 3 not ruled out.

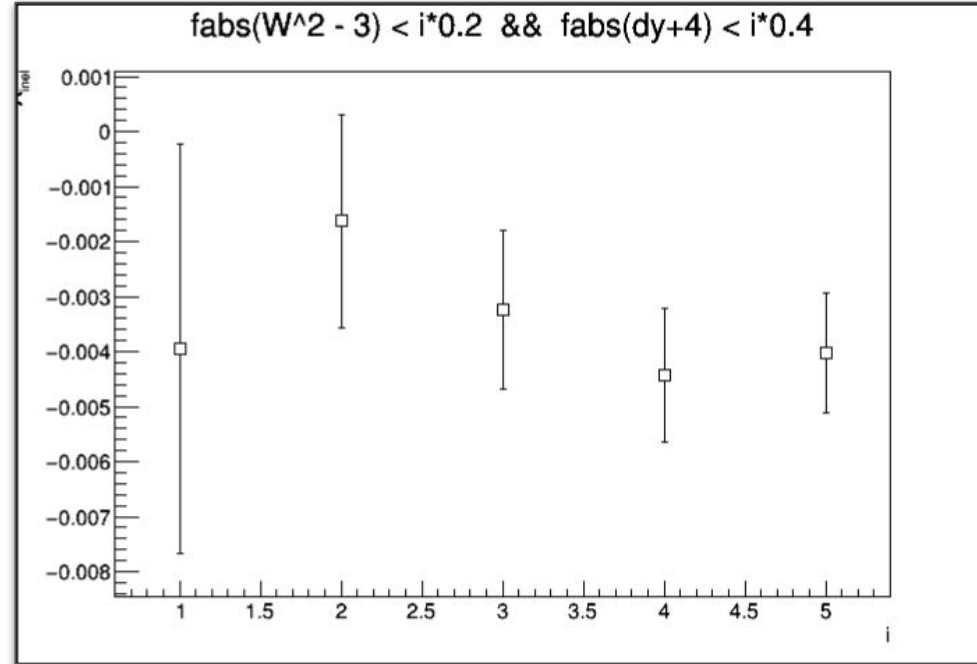
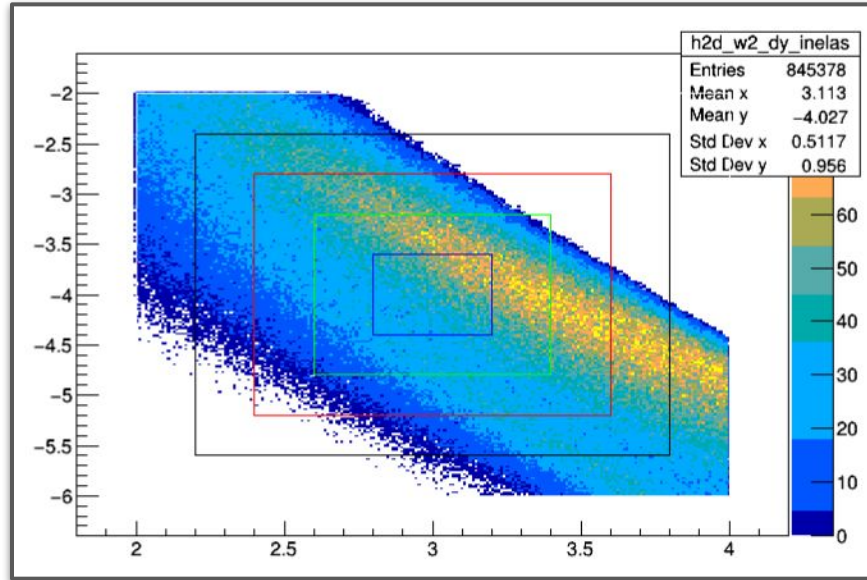
**THANKS!**



# Backup



# Preliminary Asymmetries and Backgrounds



In Progress analysis of background fractions and associated dilution asymmetries

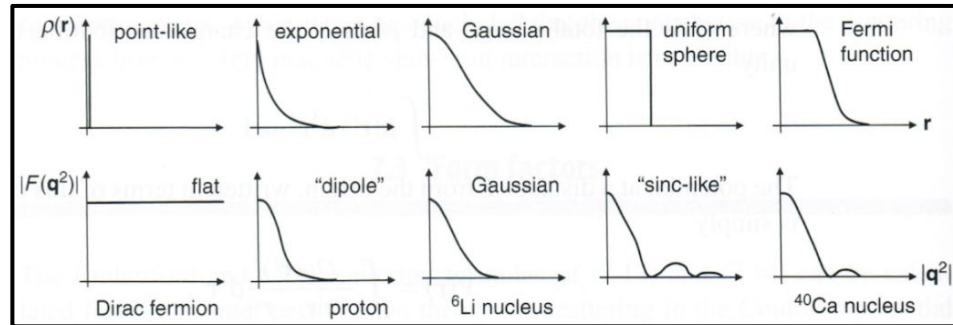
# What Is A Form Factor?

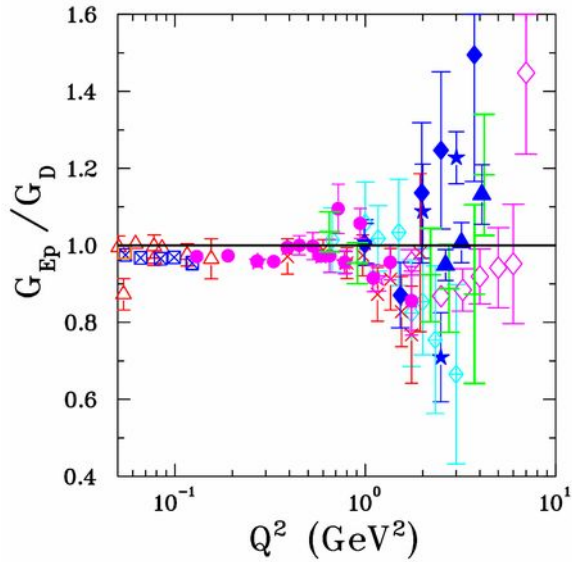
Generally, a form factor is just a fourier transform of a charge distribution:

$$F(\vec{q}) = \int d^3r \rho(r) e^{i\vec{q}\cdot\vec{r}}$$

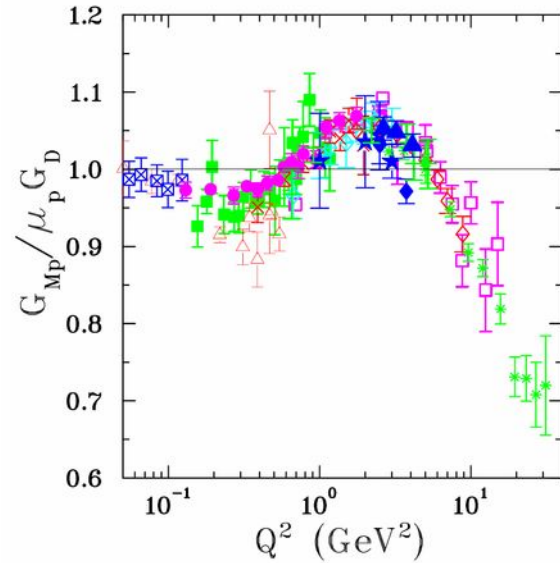
Elastic Form Factors  $G_E$ ,  $G_M$  Describe internal structure of nucleons.

Related to charge and magnetization distributions within the nucleon.





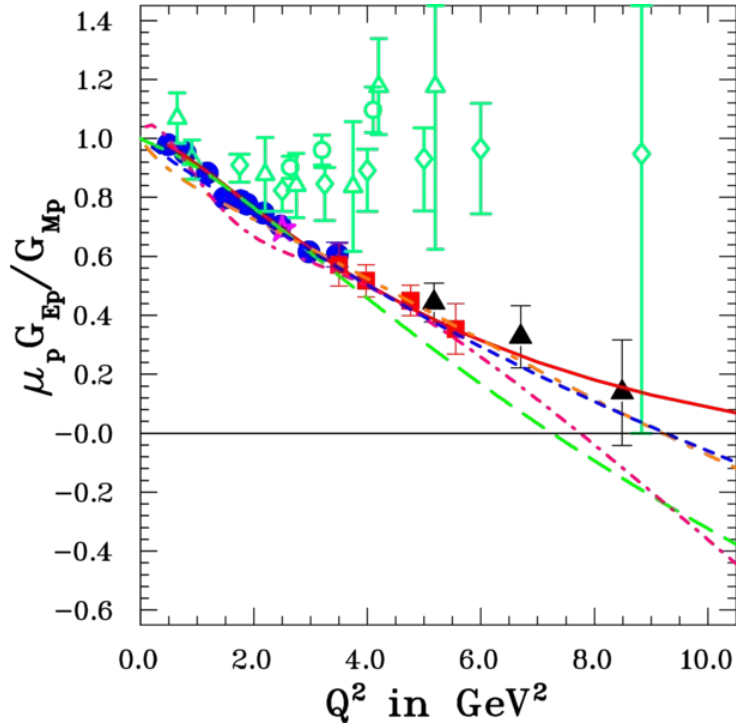
- |                      |                         |
|----------------------|-------------------------|
| $\triangle$ Hand     | $\boxtimes$ Borkowski   |
| $\blacklozenge$ Litt | $\square$ Simon         |
| $\bullet$ Price      | $\diamond$ Andivahis    |
| $\times$ Berger      | $\star$ Walker          |
| $\diamond$ Bartel    | $+$ Christy             |
| $\star$ Hanson       | $\blacktriangle$ Qattan |



- |                         |                         |
|-------------------------|-------------------------|
| $\triangle$ Hand        | $\diamond$ Bartel       |
| $\blacksquare$ Janssens | $\boxtimes$ Borkowski   |
| $\square$ Coward        | $\ast$ Sill             |
| $\blacklozenge$ Litt    | $\diamond$ Andivahis    |
| $\bullet$ Price         | $\star$ Walker          |
| $\times$ Berger         | $+$ Christy             |
| $\star$ Hanson          | $\blacktriangle$ Qattan |

Global Database for proton form factors obtained via Rosenbluth Separation method.  
 Neutron form factors much less well understood - no free neutron targets!

# Proton FFs in Double Polarisation Experiments

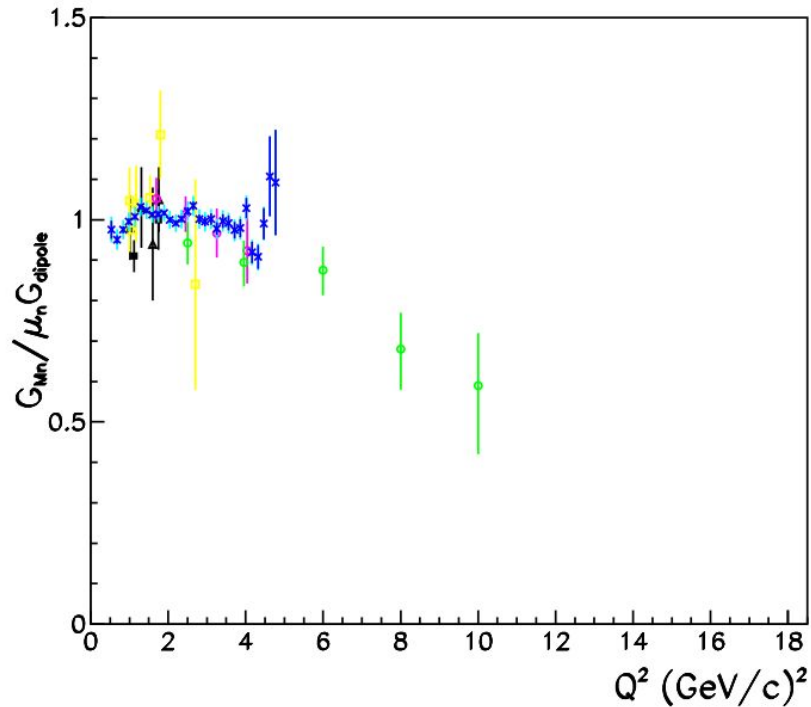


Recoil Polarisation techniques are a more sensitive way to measure  $G_p^E$  which is multiplied by  $G_p^M$  in the transverse component of the polarization,  $P_T$ .

Unlike the Rosenbluth Method, the cross section is not increasingly dominated by  $G_M^2$  at large  $Q^2$ .

World data for  $\mu G_p^E / G_p^M$  is shown on the left.

# Magnetic Form Factor of the Neutron (GMn)

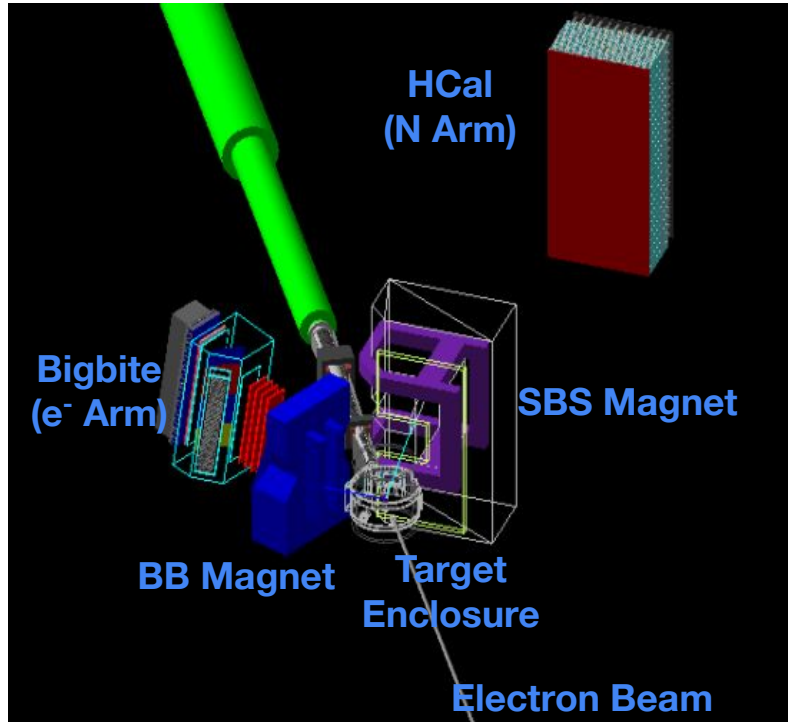


Existing data for  $G_{Mn}$  ( $Q^2 > 1 \text{ GeV}$ ), plotted as ratio to scaled dipole approximation.

Blue - CLAS e5 run, green + magenta - SLAC, yellow - old/legacy

SBS should have reduced systematic uncertainty at high  $Q^2$  in part due to ratio method.

# Hall A: Super Bigbite Spectrometer (SBS)



2 arm spectrometer - large  $\bar{x}, \bar{p}$  acceptance!

High precision form factor measurements

Installed 2020/21

First experimental run 2021/22 (GMn)

Polarised <sup>3</sup>He target installed 2022

First <sup>3</sup>He run 2022/23 (GEn) completed

Future experiments GEn-RP, Pion SDPO, GEp-V - extend in to 2025

# Spin Exchange Optical Pumping (SEOP)

Alkali vapor polarized by optical pumping from laser radiation.

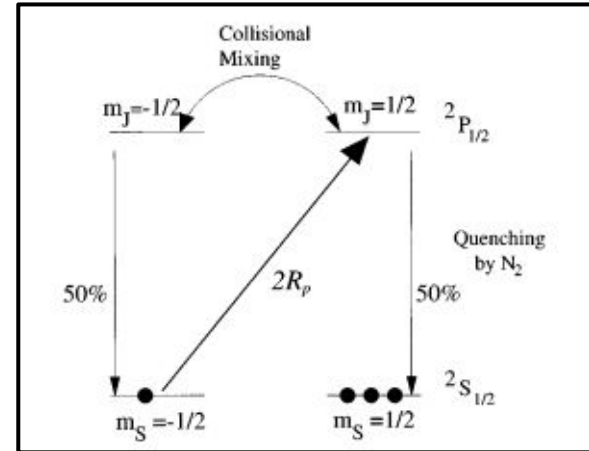
Collide with  $^3\text{He}$  transferring spin via hyperfine interactions

$$P_{\text{He}}(t) = P_{\text{Alk}} \frac{\gamma_{se}}{\gamma_{se}(1+X) + \Gamma} (1 - e^{-t(\gamma_{se} + \Gamma)})$$

Nitrogen Suppresses reradiation via quenching of excited atoms

Mix of Kb and K increases **efficiency** of polarization of the helium

High power diode lasers allow for larger **volume** of helium to be polarized



# Nuclear Magnetic Resonance (NMR)

- Apply RF field to spins
  - Resonance → Signal in Coils
- Meet Resonance Criteria Via Adiabatic Fast Passage (AFP)

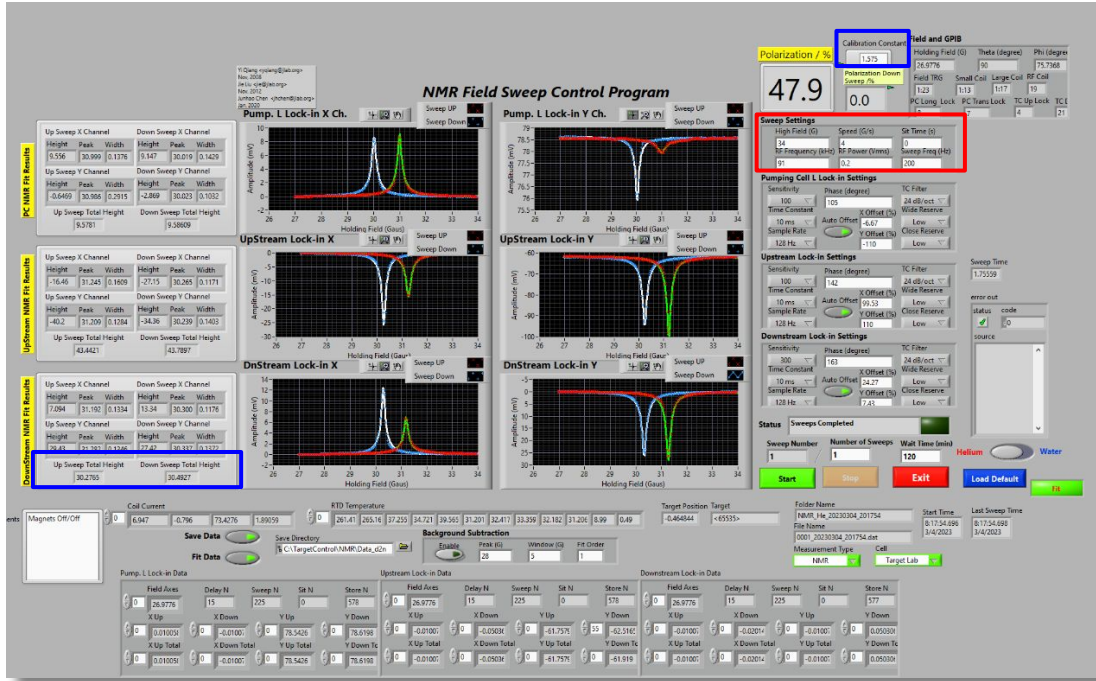
• Destructive measurement - AFP sweeps cause losses ~1%

• mV:% conversion factor required to get true polarisation value

$$D_x = \frac{US_x + DS_x}{2} \quad D_y = \frac{US_y + DS_y}{2}$$

$$D = \sqrt{D_x^2 + D_y^2}$$

$$S_{NMR} \approx D$$



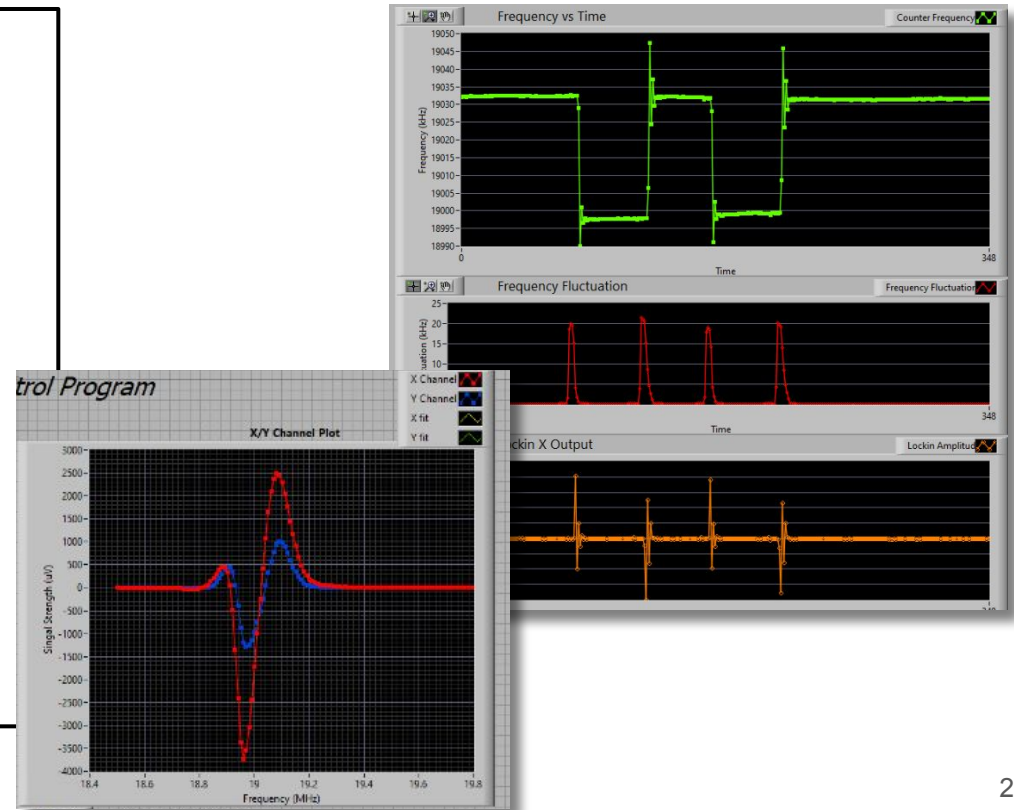


# Electron Paramagnetic Resonance (EPR)

## EPR - Measure Zeeman Effect in K electrons

- Frequency sweep over alkali resonance modes
  - Signal when frequency == splitting.
- Signal is first derivative of absorption spectrum
- EPR non destructive - AFP still causes losses.

$$c = \frac{S_{\text{NMR}}}{P_{\text{EPR}}(n_p \Phi_p + n_t \Phi_t + n_{tt} \Phi_{tt})}$$



$$\sigma_h = \Sigma + h\Delta$$

$$A_N = \frac{\sigma_+ - \sigma_-}{\sigma_+ + \sigma_-} = \frac{\Delta}{\Sigma}$$

$$\Sigma = \frac{d\sigma}{d\Omega} \Big|_{\text{Mott}} \frac{E_f}{E_i} \left( \frac{G_E^2 + \tau G_M^2}{1 + \tau} + 2\tau G_M^2 \tan^2(\theta/2) \right)$$

$$\Delta = -2 \frac{d\sigma}{d\Omega} \Big|_{\text{Mott}} \frac{E_f}{E_i} \sqrt{\frac{\tau}{1 + \tau}} \tan(\theta/2) \left[ \sqrt{\tau(1 + (1 + \tau) \tan^2(\theta/2))} \cos \theta^* G_M^2 + \sin \theta^* \cos \phi^* G_M G_E \right]$$

$$A_{\text{phys}} = - \frac{2\sqrt{\tau(\tau + 1)} \tan(\theta/2) G_E^n G_M^n \sin \theta^* \cos \phi^*}{(G_E^n)^2 + (G_M^n)^2 (\tau + 2\tau(1 + \tau) \tan^2(\theta/2))} - \frac{2\tau \sqrt{1 + \tau + (1 + \tau)^2 \tan^2(\theta/2)} \tan(\theta/2) (G_M^n)^2 \cos \theta^*}{(G_E^n)^2 + (G_M^n)^2 (\tau + 2\tau(1 + \tau) \tan^2(\theta/2))}$$

$$A_{\perp} = - \frac{G_E^n}{G_M^n} \frac{2\sqrt{\tau(\tau + 1)} \tan(\theta/2)}{(G_E^n/G_M^n)^2 + (\tau + 2\tau(1 + \tau) \tan^2(\theta/2))}$$